



Risk assessment of glacial lake outburst flood in the Central Asian Tianshan Mountains



Man Chen¹, Yaning Chen¹ , Gonghuan Fang¹ , Guoxiong Zheng³, Zhi Li¹ , Yupeng Li² & Ziyang Zhu²

Global warming has accelerated alpine glacier melting and led to an increased risk of glacial lake outburst floods (GLOFs). This paper extracted glacial lake boundaries in the Tianshan Mountains of Central Asia from 1990 to 2023, analyzed their spatiotemporal variations and evaluated their risk levels under current and future scenarios. The results show that glacial lakes are predominantly distributed in the Central and Western Tianshan, accounting for 75% of the total number in the Tianshan region. The number and area of glacial lakes increased by 148% (from 1837 to 4557) and 71.83% (from 119.73 to 205.73 km²) during 1990 to 2023, with moraine lake expansion predominating. In the Western Tianshan, the high or very high risk of GLOF is 3–4 times that of other areas. By the middle of the twenty-first century, GLOF risk will continue to increase, especially in the Western Tianshan. This study can provide scientific foundation for disaster mitigation in the downstream areas.

Glacial lake outburst floods (GLOFs) are a sudden, hazardous, and wide-ranging natural disaster phenomena, often accompanied by mudslides¹. They mainly occur as outburst floods triggered by glacial lake dam failure in high alpine mountains. The result is a rapid release of large quantities of water and sediments, with the sudden deluge often proving disastrous for downstream areas, damaging both the natural and socio-ecological environments².

Over the past half-century, global warming has spurred glacier retreats^{3,4}. At the same time, climate change has led to the rapid expansion of glacial lakes and the further formation of new ones. This expansion is particularly noticeable in alpine mountains, where the area and water volume of the lakes are increasing. Unfortunately, the increase in size also brings with it an increase in the risk of GLOFs².

On the one hand, GLOFs can provide a valuable water resource and hydroelectric power to downstream areas, which is of great significance to the production and life of residents downstream. However, on the other hand, they can also cause major destruction to residential homes and other infrastructure. The damage can extend for thousands of kilometers from the headwaters to downstream areas^{5,6}. Furthermore, the occurrence of GLOFs has significant implications for the spatial and temporal distribution and utilization of water resources in alpine regions⁷.

Glacial lakes are highly susceptible to climate change, and their worldwide increase in number, size, and volume can mainly be

attributed to global warming, with additional contributions from other climatic drivers (e.g., extreme hydrologic events, human activities, and glacier changes). From 1990 to 1999, 9414 glacial lakes (>0.05 km²) globally covered $\sim 5.93 \times 10^3$ km² of Earth's surface. As of 2015 to 2018, the number and volume of glacial lakes globally increased by 53% and 48% over 1990 to 1999, respectively, for a total of $\sim 14,394$ lakes and a coverage of 8.95×10^3 km² in area^{8,9}. However, the growth distribution of glacial lakes is not uniform and displays major regional differences. For instance, the growth in area and capacity of high-altitude glacial lakes saw a rapid expansion, which is consistent with the effects of global warming. This type of growth dominated high-altitude regions such as Alaska, Greenland, and the Third Pole. Glacial lakes in High Mountains Asia (HMA) have been studied that glacial lakes in HMA are relatively small at high latitudes, but are growing rapidly in some sub-regions. Between 1990–1999 and 2015–2018, the lake volume in the entire region increased by $\sim 45\%$, to 4.6 km³. The number of lakes in the Asia South East region, including Nepal, northern India, Bhutan, and a part of southwestern China, has nearly doubled^{10–12}.

Moraine and ice dam lakes are the main sources of sudden GLOF events. Factors such as ice-rock avalanches, extreme precipitation, glacial ice melting, and other destabilizing forces can weaken the dam body, causing the moraine dam pipe to rupture. The resulting rapid release of a large amount of water from the lake creates the GLOF disaster^{13,14}. Since 1990, the

¹College of Geographic Science and Tourism, Xinjiang Normal University, Urumqi, China. ²State Key Laboratory of Desert and Oasis Ecology, Key Laboratory of Ecological Safety and Sustainable Development in Arid Lands, Xinjiang Institute of Ecology and Geography, Chinese Academy of Sciences, Urumqi, China.

³College of Earth and Environmental Sciences, Lanzhou University, Lanzhou, China. e-mail: chenyn@ms.xjb.ac.cn; fanggh@ms.xjb.ac.cn

area and number of glacial lakes in high mountainous regions around the world have shown a general trend of increase. GLOFs recorded in most glaciated mountain areas worldwide have increased. The ongoing glacier melting and the expansion of glacial lakes are expected to further increase the frequency of GLOFs. With the anticipated warming in the future, the risk of GLOFs is also expected to increase¹⁵. Taylor et al. studied the damage potential and spatial distribution characteristics of outburst flooding on a global scale, showing that 15 million people worldwide are affected by potential GLOFs, with most of the exposed populations living in the high mountain regions of Asia². Zheng et al. demonstrated that in the Third Pole region, GLOF risk is concentrated in the eastern Himalayas and that current risk levels are at least twice those of neighboring areas¹⁶. For instance, in the Karakoram region, many glaciers are experiencing frequent, irregular, and sudden advancement. This phenomenon could potentially lead to a future increase in GLOFs across the Karakoram Mountains¹⁷. Carrivick et al. employed various indicators combined with the global assessment of GLOF's social impact, concluding that the occurrence of this mountain disaster is mainly related to glacier mass balance and climate^{18,19}.

The Tianshan Mountains are situated in Central Asia. It stretches about 2500 km across the central part of the Eurasian continent and has an average elevation of over 3500 m. Commonly referred to as the "Water Tower of Central Asia", the Tianshan Mountains are home to a vast area of modern glaciers (Fig. 1). This region is also known for having a high frequency of GLOFs, which, according to reports, are mainly caused by moraine and ice-dammed lakes.

The outburst of glacial lakes typically triggers a series of other natural disasters, such as mudslides and landslides, which are among the most serious threats to the region. Previous studies of glacial lakes in the Central Asian mountain range have primarily focused on the dynamic evolution of specific active glacial lakes, such as Lake Mazhabach²⁰, along with the identification of potentially hazardous glacial lakes and the reconstruction of GLOFs^{21,22}. The current warming rate is 0.36~0.42 °C/10a and the increase rate of precipitation is around 8.4 mm/10a⁷. Consequently, glacier ablation

has accelerated²³, exacerbating the potential risk of GLOF-induced disasters (Fig. 2).

This paper provides a comprehensive mapping and classification of glacial lakes with an area larger than 0.01 km² in the Tianshan Mountains using remote sensing imagery. The current and future outburst flood risk were then analyzed. The objective of this research is to analyze the spatial and temporal variations of glacial lakes and to evaluate the risk of future GLOF events in the context of climate change. The paper focuses on the following three aspects: (1) uncovering trends in the number and area of glacial lakes over the past 30 years using remote sensing images; (2) quantifying the hazard and risk level of glacial lakes based on an improved risk assessment model for the current and future period; and (3) analyzing future risk by combining glacier thickness data and GloGEM model data.

Results

Historical spatiotemporal changes of glacial lakes

The total number of glacial lakes was 4557, with a total area of $205.73 \pm 0.17 \text{ km}^2$ in 2023. The glacial lakes were mainly concentrated in the Central Tianshan (with a number of 1870 glacial lakes), Western Tianshan (1548 glacial lakes), followed by Northern and Eastern Tianshan. Of these 4557 lakes, over half (~54.29%) were moraines, with a total area of $87.95 \pm 0.1 \text{ km}^2$.

The number and area of glacial lakes increased significantly between 1990 and 2023. The number of glacial lakes increased by 2720 (~148%), and the area expanded by 71.83%. From 1990 to 2000, the number of glacial lakes increased by 29.94% and the area expanded by $7.02 \pm 0.17\%$. From 2000 to 2010, the number and area of glacial lakes increased by 24.17% and $19.78 \pm 0.19\%$, respectively, while the number and area of glacial lakes increased by 28.54% and $17.40 \pm 0.18\%$ from 2010 to 2020, respectively. From 2020 to 2023, the number and area of glacial lakes increased by 19.6% and $14.18 \pm 0.17\%$, respectively.

Spatially, the Central Tianshan had the highest growth in both the number and area of glacial lakes from 1990 to 2023, with an increase of 188%

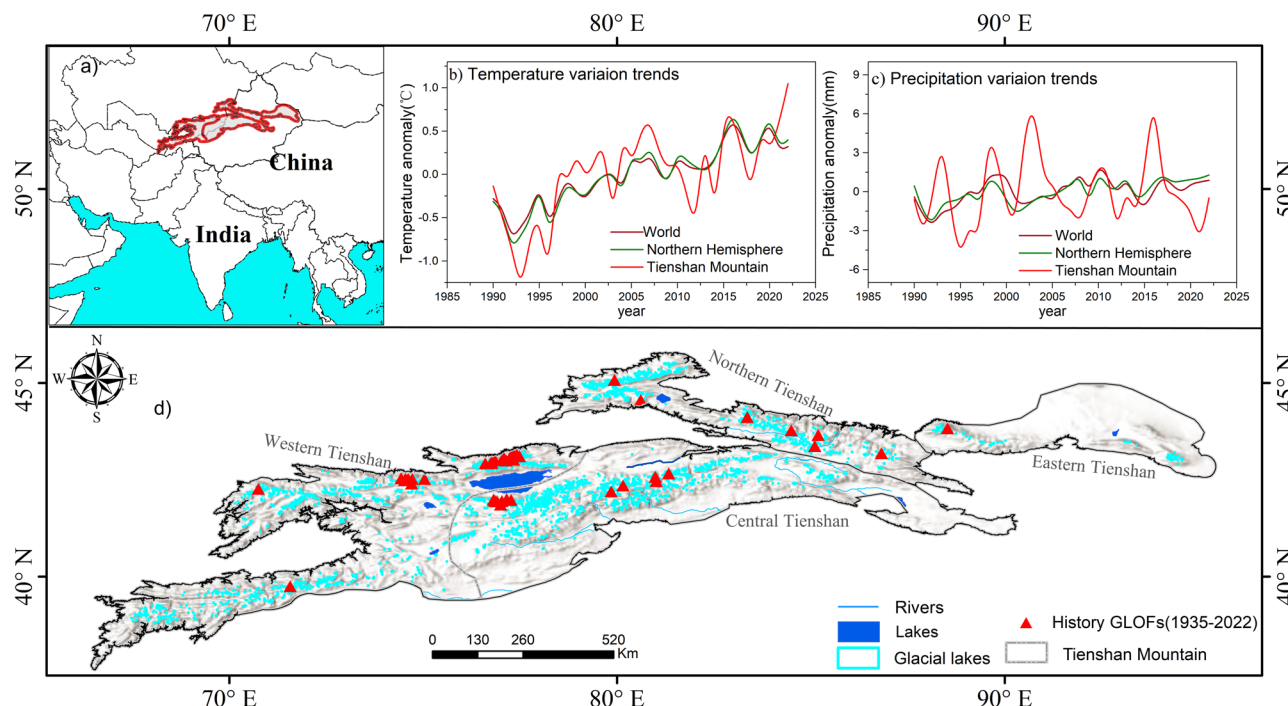


Fig. 1 | Location of the study area. **a** The location of the Tianshan Mountains in Central Asia. **b, c** The mean annual temperature and mean annual precipitation trends from 1990 to 2022 globally, in the northern hemisphere, and in the Tianshan Mountains. The maroon line represents global trends, the green line represents the Northern Hemisphere, and the red line represents the Tianshan

Mountains. **d** The distribution of glacial lakes in the Central Asian Tianshan Mountains. Red triangles represent GLOFs in the Tianshan Mountains from 1923 to 2022; the blue lines represent Rivers, the blue-filled boxes represent lakes, and the light blue boxes represent glacial lakes; historical GLOFs represent the record of past GLOF events.

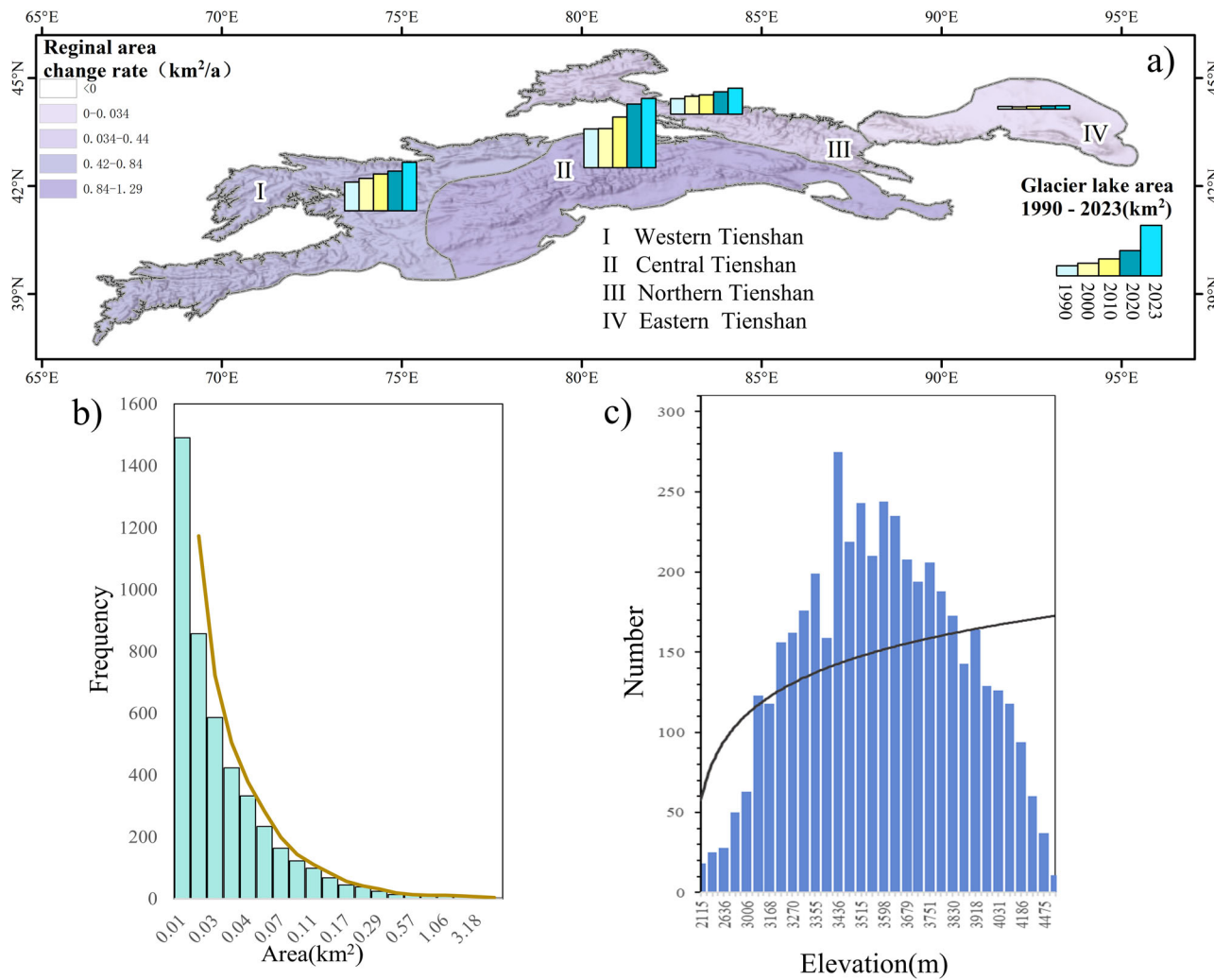


Fig. 2 | The area of glacial lakes distributed in the Tianshan Mountains. a The maps highlight the expansion rate of glacial lakes between 1990 and 2023 (areas $\geq 0.01 \text{ km}^2$). The bars, which vary in color and size, represent the rate of glacial

lake area expansion and the total area of glacial lakes in the study area. The size of the bars indicates the glacial lake area in 2023. The histograms present the frequency of the glacial lakes in terms of their size (b) and elevation (c).

Table 1 | Statistics of glacial lakes in different regions of the Tianshan Mountains from 1990 to 2023

Year	Western Tianshan Area/km ² (lake number)	Northern Tianshan Area/km ² (lake number)	Central Tianshan Area/km ² (lake number)	Eastern Tianshan Area/km ² (lake number)	Total Area/km ² (lake number)
1990	40.11 ± 0.21 (631)	21.84 ± 0.07 (488)	54.13 ± 0.3 (650)	3.65 ± 0.05 (68)	119.73 ± 0.23 (1837)
2000	45.22 ± 0.22 (768)	25.01 ± 0.06 (612)	54.64 ± 0.17 (928)	3.26 ± 0.05 (79)	128.13 ± 0.17 (2387)
2010	51.47 ± 0.19 (1000)	27.25 ± 0.06 (710)	70.87 ± 0.24 (1168)	3.88 ± 0.05 (86)	153.47 ± 0.19 (2964)
2020	55.42 ± 0.18 (1199)	31.36 ± 0.05 (872)	88.98 ± 0.22 (1639)	4.42 ± 0.06 (100)	180.18 ± 0.18 (3810)
2023	67.75 ± 0.16 (1548)	36.41 ± 0.05 (1018)	96.80 ± 0.2 (1870)	4.77 ± 0.06 (121)	205.73 ± 0.17 (4557)

in glacial number and $78.83 \pm 0.3\%$ in the lake area. Western Tianshan followed closely behind, with the number of glacial lakes increased by 45.32% and the area increased by $68.91 \pm 0.16\%$. The expansions of glacial lakes in Northern and Eastern Tianshan, however, were relatively moderate, with the relative increments in glacial lake area being $66.71 \pm 0.05\%$ and $30.68 \pm 0.06\%$, respectively (Table 1).

Historical GLOF events

Over the past two centuries, the Tianshan region has experienced at least 234 GLOFs in 49 glacial lakes. We collected and analyzed the records of these events to better understand their spatial distribution and attribute characteristics. The data are based on the Asian alpine glacial lake outburst event

dataset and were primarily derived from previous research and relevant news reports (Fig. 3).

Among the 49 glacial lakes, 40 glacial lakes were moraine-dammed lakes. There have been 122 moraine-dammed lake outburst flood events, accounting for 52% of the total number of GLOFs (Fig. 3a). There were 93 GLOF events occurred in ice-dammed glacial lakes (i.e., the Merzbacher Lake)¹⁶, whereas only 19 events happened in other types of glacial lakes. Spatially, 96% of the total number of GLOFs was happened in the Western and Central Tianshan.

As the GLOFs originating in ice-dammed lakes, such as the Merzbacher Lake, are often cyclical and high frequency, this study did not include these types of lakes. In the following section, only 122 GLOFs in 40 moraine-

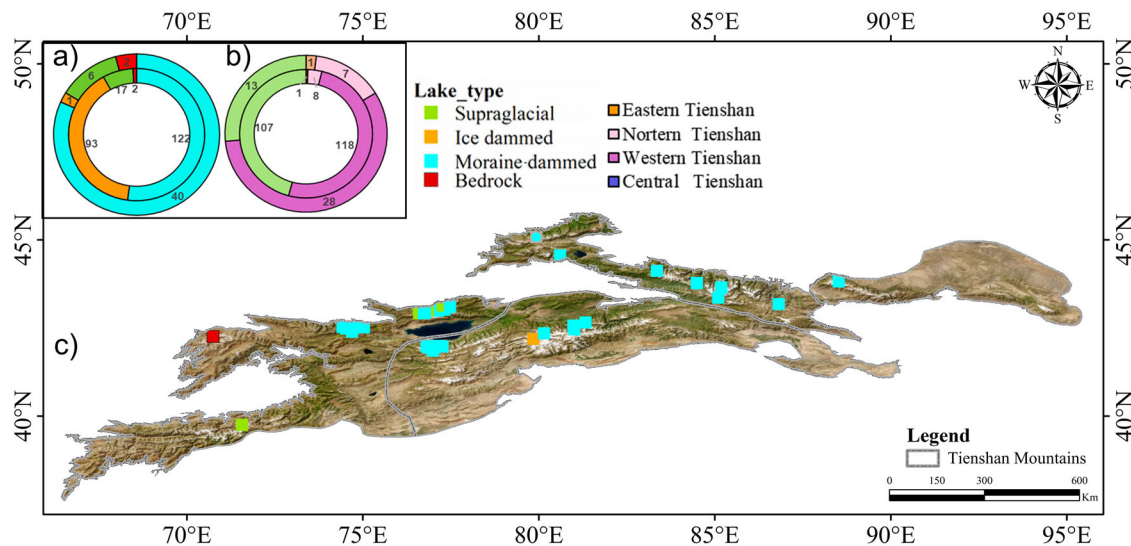


Fig. 3 | Historical GLOFs in the Tianshan Mountains. **a** A double doughnut chart illustrates the number of past GLOF sources (outer circle) and the frequency of floods (inner circle), categorized by different types of lakes. **b** Another double doughnut chart delineates the number of past GLOF sources (outer circle) and the

frequency of floods (inner circle) in different regions of the Tianshan Mountains. **c** Depict the spatial distribution of recorded GLOF sources, which are classified according to the type of Lake Dam.

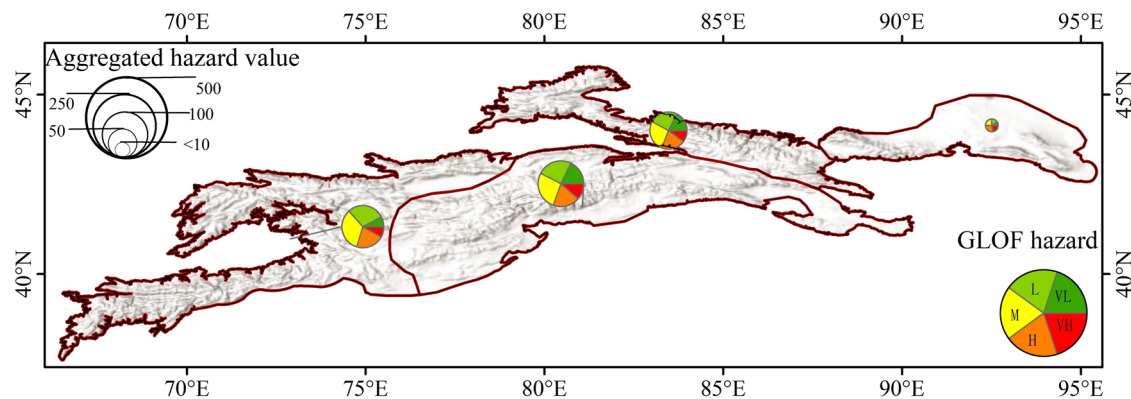


Fig. 4 | Pie charts showing the proportion of different GLOF hazard levels in the current period (year 2023). VH very high, H high, M medium, L low, and VL very low.

dammed glacial lakes were used for the validation of the glacial risk assessment model.

Risk assessment of GLOFs in the current period

In this research, a total of 2474 moraine lakes in the Tianshan Mountains in 2023 were quantitatively assessed for their potential GLOF hazard and risk levels, based on the improved GLOF risk assessment model¹⁶. For GLOF exposure level, ~97.73% of the investigated lakes have a low or very low exposure level due to the lack of significant downstream infrastructure within the flood paths of the region. For GLOF hazard level, 512 and 253 moraine-dammed lakes are considered to have high or very high hazard levels of GLOF, accounting for ~30.92% of the total moraine-dammed lakes (Fig. 4). Spatially, approximately 38.17% (~292) and 31.37% (~240) of the high or very high-level hazard lakes are identified in the Central and Western Tianshan (Table 2). There are only 37 high or very-high hazard lakes, accounting for 4.84% of the total, located in the Eastern Tianshan.

For GLOF risk level, over one-fifth (551 lakes) of all the assessed moraine-dammed lakes in the study area had either high or very-high risk levels, whereas 39.89% (987) were at low or very-low risk. The low and very-low risks of GLOF are mainly due to a lack of significant downstream infrastructure within the flood paths of the region (Fig. 5). The low and very-low risks of GLOF are mainly due to their low exposure level. It is worth

noting that the current high or very-high risk levels of GLOFs are still in the Western and Central Tianshan, accounting for 51.36% (283) and 31.40% (173).

The GLOF risk assessment model was validated against recorded GLOF events in 40 marine-dammed lakes. The hazard level of GLOF represents the potential extent to which such floods might occur, whereas the risk level takes into account both the hazard level of the GLOF and their potential impact on downstream areas. In other words, the risk level jointly considers both the hazard level and the potential impact of the floods (reflected by the exposure level). The results show that the hazard assessment model used in this paper successfully identified 32 of the 40 moraine-dammed lakes with previous GLOF as having high or very-high hazard levels. The simulation had an assessment accuracy of 80%, which demonstrates the high reliability of the model (Fig. 6).

Risk assessment of future GLOF events

By 2050, under the high emission scenario (RCP8.5), additional 1140 glacial lakes with an area of more than 41.94 km^2 are likely to form (Fig. 7). Under the medium-low emission scenarios (RCP4.5, RCP2.6), the areas of additional glacial lakes are forecasted to be approximately 36.67 and 30.57 km^2 . By 2100, the newly expanded areas of glacial lakes will potentially reach to 108.87, 79.00, and 55.82 km^2 under RCP8.5, RCP4.5,

and RCP2.6 (Table 3). These newly formed glacial lakes are predicted to form predominantly in the Central and Western Tianshan. Meanwhile, the number, area, and volume of lakes across the Tianshan Mountains will continue to expand under the three emission scenarios by the end of the twenty-first century. Under the future scenario of complete glacier ablation (i.e., ice-free scenario), 2441 new glacial lakes may be formed in these regions, for a total area of about 136.1 km² and an overall volume of about 22.69 km³.

The future GLOF risk was assessed using the improved risk assessment model in the Tianshan Mountains. By 2100, the hazard values for moraine-dammed lakes are expected to increase by a factor ranging from 0.44 to 1.22 (Fig. 8). However, the risk values are projected to decrease by 39%~99% of their current levels within the same period. Spatially, ~57.99% of the lakes in the Central Tianshan are forecasted to have high or very-high levels of hazard values, followed by Western Tianshan (~27.45%) and Eastern Tianshan (Fig. 9).

Table 2 | Hazard level, exposure level, and risk levels of moraine lakes in the Tianshan in 2023

Region	Class-level	Exposure level (lake number)	Hazard level (lake number)	Risk level (lake number)
Western Tianshan	Very low	741	64	126
	Low	21	230	172
	Medium	7	272	226
	High	25	175	198
	Very high	12	65	84
Central Tianshan	Very low	924	172	407
	Low	24	235	200
	Medium	5	260	180
	High	5	183	110
	Very high	1	109	62
Northern Tianshan	Very low	631	111	287
	Low	2	156	159
	Medium	1	171	121
	High	0	133	52
	Very high	0	63	15
Eastern Tianshan	Very low	61	7	25
	Low	14	12	7
	Medium	0	19	13
	High	0	21	11
	Very high	0	16	19

The number of future moraine-dammed lakes anticipated being high and very-high risk would increase from the current 551 to approximately 760 and 948 in 2050 and 2100, respectively. Under the ice-free scenario, the number of future moraine-dammed lakes with high or very-high risk levels will increase to 1040. Considering future changes in population, infrastructure, and tourism, which are gradually expanding into the alpine zones, it is likely that the exposure level will increase^{1,17}.

Overall, the Western and Central Tianshan are anticipated to have the highest risk values of GLOF. The Central Tianshan will see the largest increase in the number of high and very-high risk moraine-dammed lakes, followed by the Western Tianshan. Eastern Tianshan is predicted to have far fewer future moraine-dammed lakes than other regions, yet 40~52% of those lakes are expected to have high or very high-risk levels, making them an area of concern (Fig. 9). Nonetheless, under all future assessment scenarios, the Western and Central Tianshan will remain the primary GLOF hotspot. Under the RCP4.5 and RCP8.5 scenarios, GLOFs in the Central and Western Tianshan are more prominent in terms of hazard level and risk level. Our analysis shows that although the hazard level of the Central Tianshan is 0.13~0.6 times higher than that of the Western Tianshan, the latter region has the highest risk level for GLOFs. This risk level is predicted to continue increasing in the future.

Discussion

Impact of different spatial resolution images on glacial lake extraction

Glacial lakes are mainly located in high-elevation mountains with wide glacier coverage, which makes human field detection difficult. Although

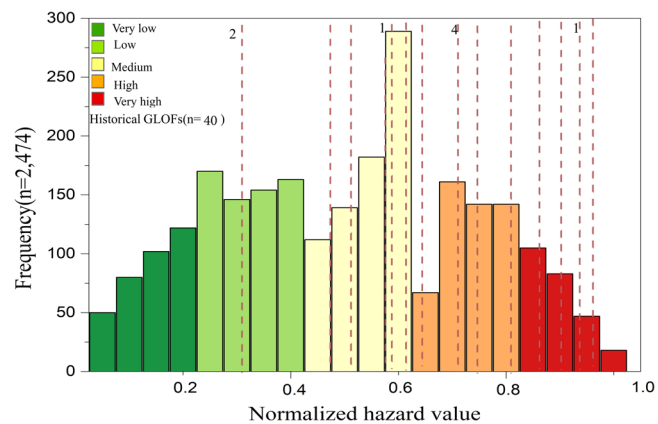


Fig. 6 | Classification of hazard level of GLOF for moraine-dammed lakes in the Tianshan Mountains. Histogram showing the distribution of GLOF hazard levels in all moraine-dammed lakes. The vertical dashed line represents the recorded historical GLOF events with estimated normalized hazard values for moraine-dammed lakes, which is used to further verify the overall model performance (VH very high, H high, M medium, L low, VL very low).

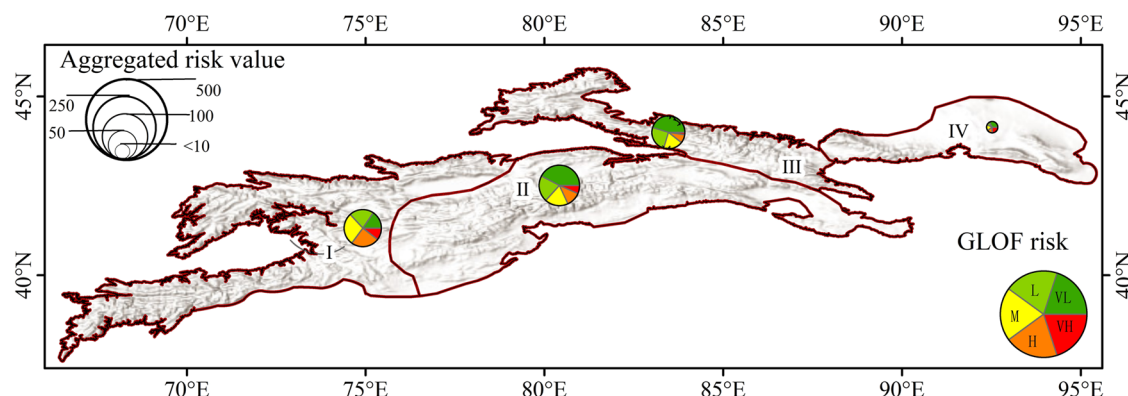


Fig. 5 | Pie charts showing the proportion of different GLOF risk levels in the current period (year 2023). VH very high, H high, M medium, L low, and VL very low.

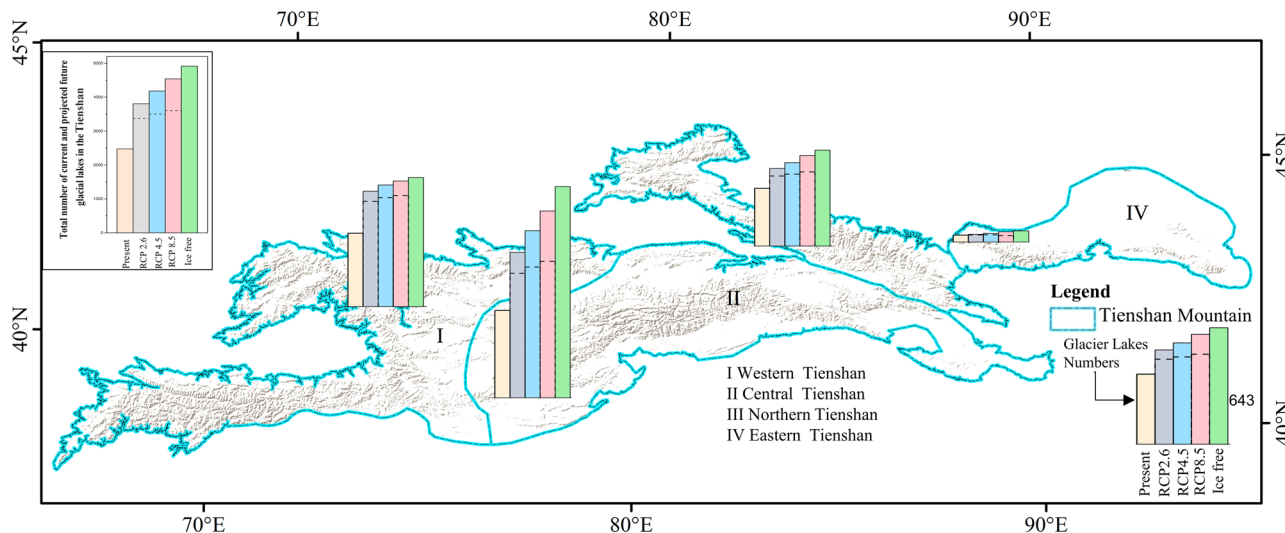


Fig. 7 | Present and projected glacial lakes in 2050 and 2100 in the Tienshan Mountains. Bar charts in different colors denote the present and projected glacial lake numbers. Dashed lines show the estimated glacial lake number in 2050. For

2100, the number of glacial lakes was shown under four scenarios, i.e., RCP2.6, RCP4.5, RCP8.5, and ice free.

Table 3 | Number and area of new glacial lakes in the Tienshan in 2050 and 2100 under different RCP scenarios

2050			2100				
Region	Area/km ² (quantity)			Area/km ² (quantity)			
	RCP2.6	RCP4.5	RCP8.5	RCP2.6	RCP4.5	RCP8.5	Ice free
Western	11.73 ± 0.68 (351)	14.07 ± 0.06 (392)	15.01 ± 0.06 (414)	17.36 ± 0.06 (463)	21.44 ± 0.06 (531)	23.94 ± 0.07 (575)	26.14 ± 0.06 (612)
Northern	3.63 ± 0.15 (136)	4.56 ± 0.15 (156)	5.78 ± 0.14 (181)	8.68 ± 0.13 (219)	14.07 ± 0.14 (283)	22.65 ± 0.17 (362)	25.75 ± 0.12 (421)
Central	15.16 ± 0.51 (409)	17.98 ± 0.48 (478)	21.09 ± 0.46 (541)	29.88 ± 0.24 (640)	42.88 ± 0.35 (877)	60.3 ± 0.32 (1093)	83.42 ± 0.34 (1361)
Eastern	0.04 ± 0.001 (3)	0.058 ± 0.01 (4)	0.058 ± 0.01 (4)	0.19 ± 0.01 (9)	0.62 ± 0.01 (18)	2.03 ± 0.08 (37)	2.56 ± 0.06 (47)

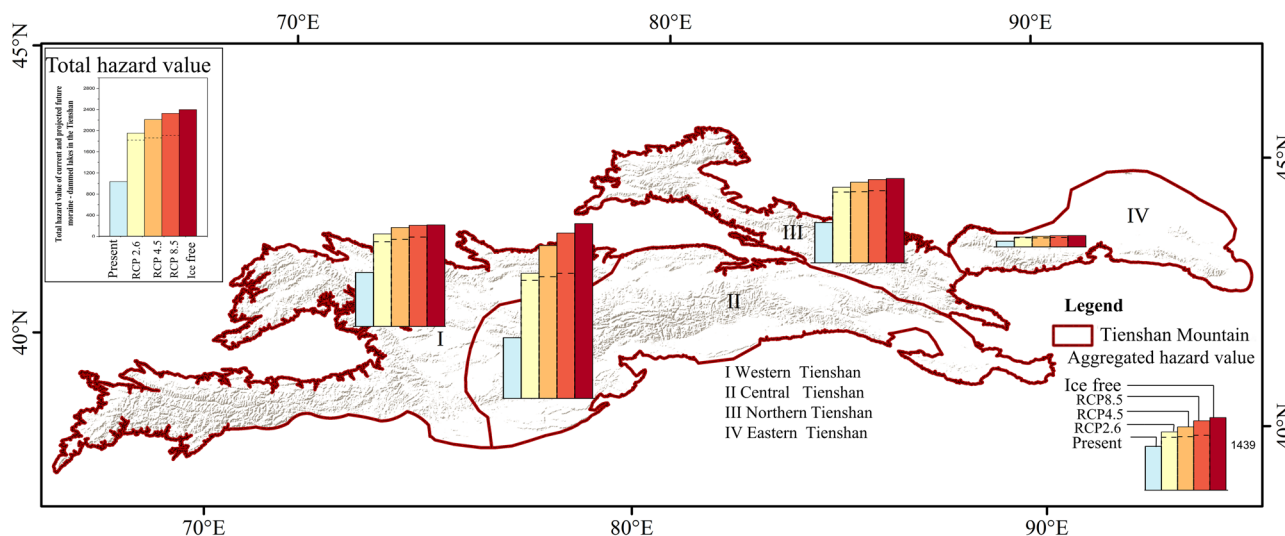


Fig. 8 | Future changes in GLOF hazard levels for 2050 and 2100, including the ice-free scenario in the Tienshan Mountains. Bar plots indicate projected changes in GLOF hazard level per region of the Tienshan Mountains from the present to 2050 and 2100 (under three RCP scenarios). Dashed lines show the hazard level in 2050.

the maturity of remote sensing technology has improved the quality of field detection data and enabled large-scale data collection, remote sensing images are still affected by a variety of factors, such as terrain shading, snow and ice, and cloud coverage. In addition, the extraction of glacial lake boundaries may be impacted by the different spatial

resolutions of images and manual visual interpretation, resulting in uncertainties²⁴.

To ensure data accuracy, this study utilized multi-source remote sensing imagery data acquired from Landsat TM, ETM+, Operational Land Imager (OLI), and Sentinel-2A/B MSI to extract glacial lake boundaries.

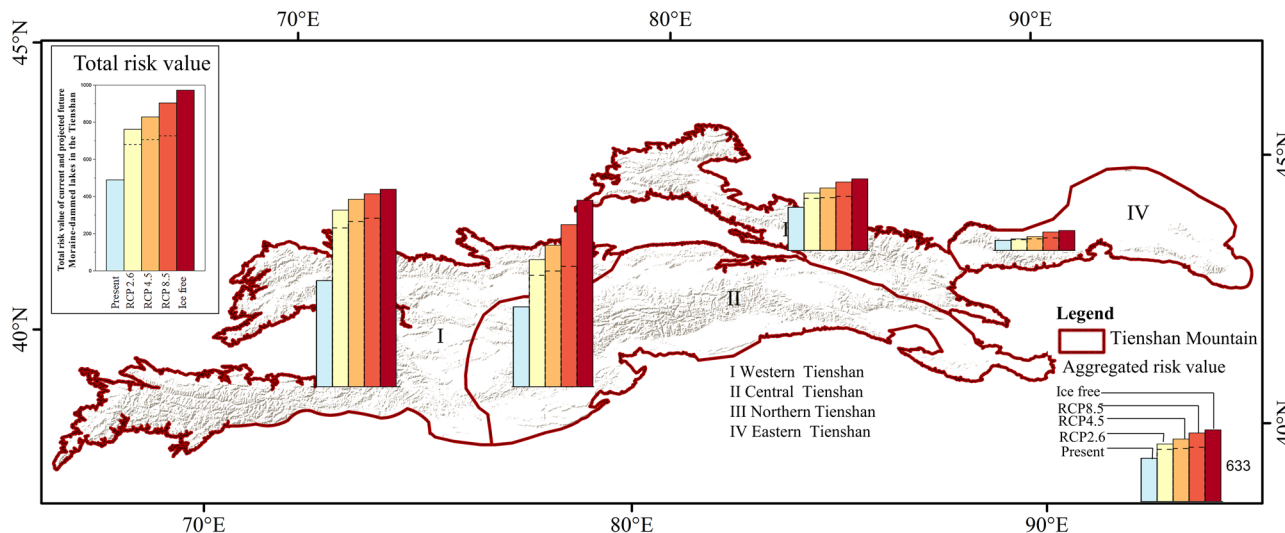


Fig. 9 | Future changes in GLOF risk levels for 2050 and 2100, including the ice-free scenario in the Tianshan Mountains. Bar plots indicate projected changes in GLOF risk level per region of the Tianshan Mountains from the present to 2050 and 2100 (under three RCP scenarios). Dashed lines show the risk level in 2050.

Table 4 | Area and uncertainty of different glacial lakes in remote sensing images with different spatial resolutions

Glacial lake	Sentinel-2 MSI 10 m		Landsat OLI 15 m		Landsat OLI 30 m	
	Area/km ²	(uncertainty/%)	Area/km ²	(uncertainty/%)	Area/km ²	(uncertainty/%)
A	2.4069	0.52	2.29768	0.61	2.3060	1.28
B	0.24008	0.14	0.24836	0.2	0.2727	0.56
C	0.178542	0.061	0.1666	0.14	0.1745	0.25
D	0.86595	0.35	0.83175	0.5	0.8434	0.78

Google Earth Engine (GEE) platform was first used for semi-automatic global-threshold segmentation extraction, and the boundaries were further refined by visual interpretation. Our method was developed on the GEE cloud computing platform, improving upon previous remote sensing data extraction techniques. This approach obtained a large remote sensing image dataset that is suitable for extracting glacial lakes at different times or seasons. The algorithm also took into account and eliminated unwanted effects such as ice, snow, clouds, and terrain shadows.

For threshold setting, we set the Modified Normalized Water Index (MNDWI) segmentation threshold at 0.01. This setting is not only highly accurate for the extraction of glacial lakes but also makes it easy to obtain the area of small glacial lakes that might otherwise be overlooked. However, because we needed to extract glacial lake data for the past three decades, which is a relatively lengthy period and includes years that pre-dating some aspects of the imagery technology we used, in extracting the 1990 glacial lake boundary, we downloaded the remote sensing images primarily by hand and performed detailed manual extraction work.

As shown in Table 4, for glacial lake A, the lower the spatial resolution, the higher the uncertainty^{9,25}. According to Sentinel-2A/B MSI, the area of glacial lake A is 2.4069 km². At a spatial resolution of 15 m, the lake area is 2.297 km² and the uncertainty is 0.61%. At a spatial resolution of 30 m, the area is 2.306 km² and the uncertainty is 1.28%. The uncertainty patterns of glacial lakes B, C, and D at different spatial resolutions are similar to the uncertainty patterns for glacial lake A (Fig. 10). The area uncertainty of the remote sensing images is all <3.5%, which is within the allowable uncertainty range. Therefore, it is completely feasible to extract the boundaries of glacial lakes from different spatial resolutions. Xie et al. have improved the accuracy of the Merzbacher Lake area extraction to over 98% through manual correction. Our experiment, completed using visual interpretation, was compared to the lake data derived from Xie et al.²⁵ in 2009 and 2010, with uncertainty of 0.04 and 0.03 km², respectively, which are <1.7%.

Driving factors of glacial lake changes

The analysis revealed that the average annual warming rate in the Tianshan Mountains (0.34 °C/10a) was higher than the global average (0.12 °C/10a). Seasonally, the warming rate was highest in spring and summer, except for the Western Tianshan, where the highest temperature increase rate is detected in winter. The higher warming rate exacerbates extreme hydrological events and injects further complexities into the water cycle in the Tianshan region^{21,26,27}. For precipitation, its magnitude is high during the summer, especially in Western and Central Tianshan. For the expansion of glacial lakes to be attributed to climate warming, a clearer understanding of how glacial lakes evolve is required, along with improved modeling of the evolutionary process and future glacier mass deficit^{10,21,28,29}.

Throughout the study period, the number, area, and volume of glacial lakes have increased rapidly worldwide, which is mainly attributed to global warming. These changes, together with other non-climatic factors, have contributed to the acceleration of glacier shrinkage and ablation. The Tianshan region in Central Asia is not only highly sensitive to global climate change but is also a hotspot for water cycle changes and home to the most developed glacial mountain range in the world^{21,23}, with a total area of glaciers in 2016 of nearly 13,566.6 km² in the Tianshan Mountains⁷.

In the context of a warm and humid climate, the melting and retreat of the glaciers will further expand glacial lakes. Changes in glacial lakes in the Tianshan region are strongly influenced by a combination of factors, such as local climate, precipitation patterns, seasonal distribution, glacier snowpack, and extreme hydrological events, making specific attribution quantification difficult. In our study, we found substantial regional variability in the growth of glacial lakes, especially in the Western Tianshan, which has the majority of the region's glaciers and glacial lakes. Overall, there is a general increasing trend of glacial lakes across the Tianshan Mountains¹³.

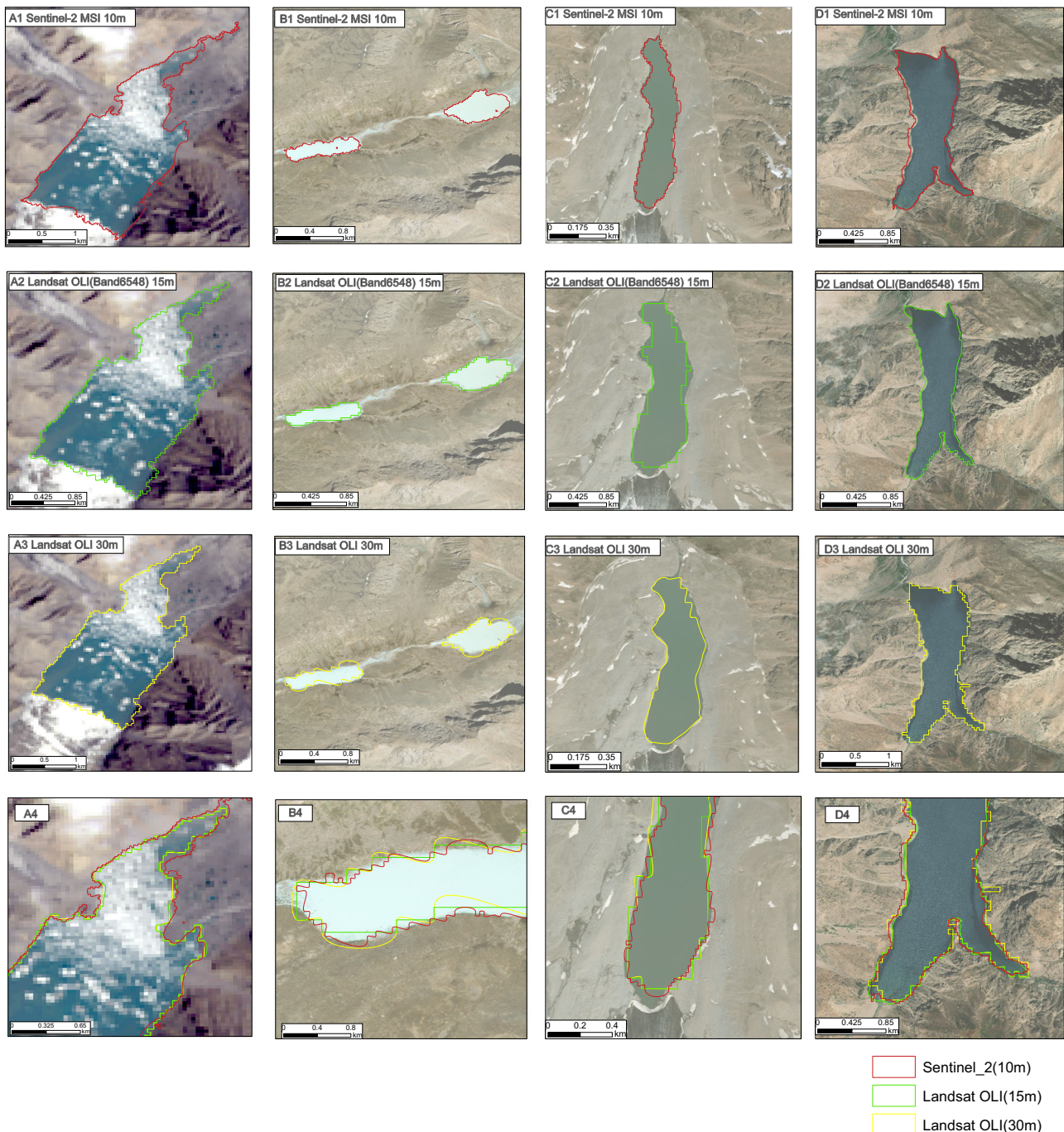


Fig. 10 | Glacial lake boundaries at different spatial resolutions. Data were collected on various dates: A1 was acquired on July 16, B1 and C1 on July 15, 2022; A2 on July 18, 2022; B2 and C2 on July 9, 2022; A3 on June 5, 2021; B3 and C3 on June 2, 2021. Additionally, A4 was acquired on July 10, 2020, and B4 and C4 were acquired

on June 25, 2020. Red borders represent Sentinel remote sensing imagery, green borders represent Landsat OLI 15 m remote sensing imagery, and yellow represents Landsat OLI 30 m remote sensing imagery.

Change in exposure index and future perspective

With the increasing number of studies on GLOFs, the GLOF research hotspots also show obvious regional differences^{3,30,31}. For the Tianshan Mountains region, most studies focused on the active glacial lakes, such as the Merzbacher Lake and at the Zyndan glacial lake in Kyrgyzstan. In this paper, we analyzed changes in glacial lakes in the four sub-regions of the Tianshan Mountains over 30 years and assessed the hazard levels, exposure levels, and risk levels of GLOFs. GLOFs can be triggered by a variety of factors, including the influx of ice/rock/meltwater into glacial lakes, the instability of morainic deposits. Additional factors influencing the likelihood and severity of GLOFs include the area and volume of the glacial lake,

the presence of strong seismic activity, and extreme hydrological conditions^{6,14}.

The risk level of GLOF will increase in the future. The hazard level of GLOF is anticipated to escalate due to accelerated glacial melt as a consequence of warming, coupled with the expansion of glacial lakes, which in turn exerts increasing pressures on the stability of the dams. At the same time, the exposure level is also expected to rise with the rapid urban development, tourism, commerce, the development of new energy, and the expansion of infrastructure into mountainous regions, as well as the population increase. The current study does not consider future changes in exposure level (assuming the future exposure level is the same as that in

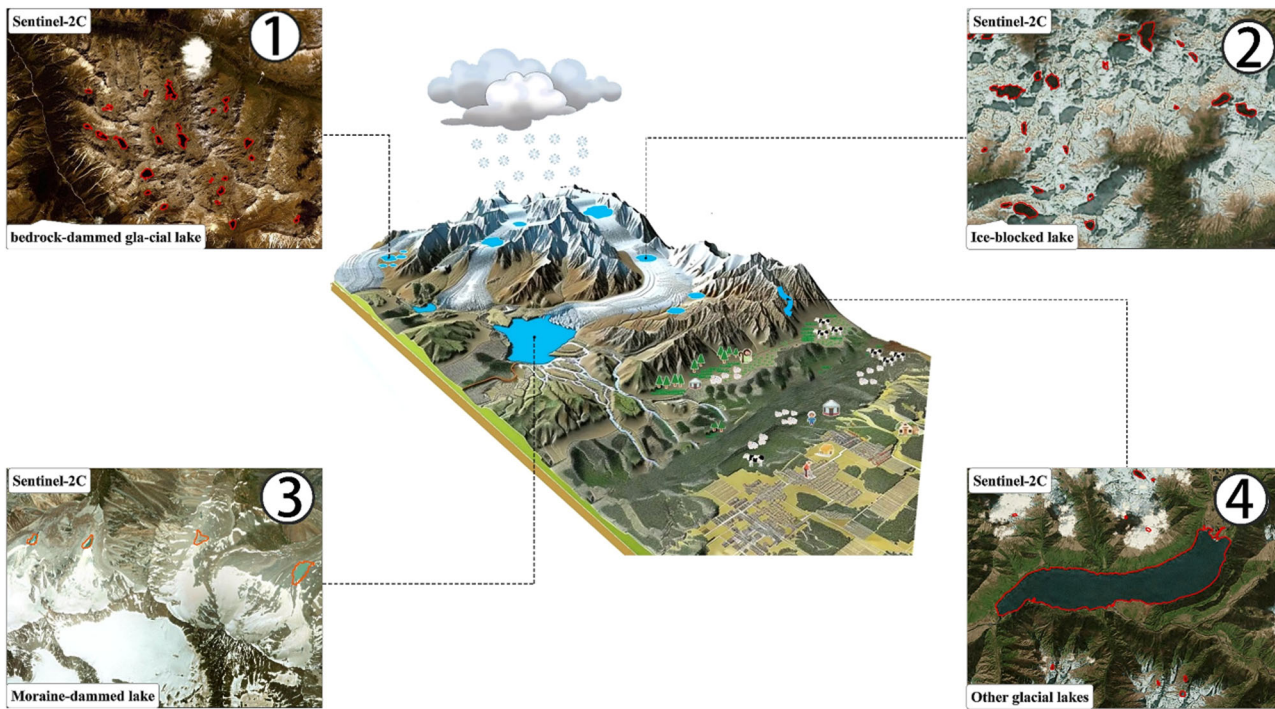


Fig. 11 | Schematic representation of glacial lake types. 1 bedrock glacial lakes, 2 ice-blocked lakes, 3 Moraine-dammed lakes, and 4 other glacial lakes (these remote images from Sentinel-MSI). These sources of the material are open access and from Canvas (<https://www.canva.cn/>).

2023), which may underestimate future GLOF risk in the high mountain areas.

Globally, 15 million people globally are exposed to impacts from potential GLOFs. Approximately 62% (amounting to 9.3 million people) of the globally exposed population are located in the high mountain regions of Asia², with high GLOF risk area distributed in the eastern Himalayas, where the risk is twice as high as in its neighboring areas¹⁶. China and Pakistan have the high risk due to the both large number of lakes and population. For the Tianshan Mountains, the hazard and exposure risk is very high compared to the Andes including Peru (Santa Basin) and Bolivia (Beni Basin), where is featured with low vulnerability. The High Arctic and Outlying Countries have the lowest GLOF risk due to low population density. GLOF risk in the Glacial Lakes inherently poses certain risks to their surrounding environments. However, the substantial volumes of water discharged from these lakes have the potential to serve as a significant water resource for downstream areas to alleviate water scarcity commonly faced by arid regions. The total volume of glacial lakes is estimated to be $\sim 4.09 \times 10^9 \text{ m}^3$ in 4557 glacial lakes in the Tianshan Mountains (the surface water resources in Xinjiang are estimated to be $74.54 \times 10^9 \text{ m}^3$), which represents 5.49% of the total surface water resources in Xinjiang. Furthermore, this can also enhance the ecological service in arid areas. The prudent management of high-risk glacial lakes necessitates the implementation of comprehensive risk assessment protocols and the establishment of early-warning systems to mitigate potential hazards^{28,32,33}.

Materials and methods

Study area

Situated in the heart of the Eurasian continent, the Tianshan Mountains connect Xinjiang in China with Kazakhstan, Kyrgyzstan, and Uzbekistan in Central Asia. The region is composed of numerous mountain ranges, basins, and modern glaciers, making it one of the world's most developed mountain systems. However, it is also vulnerable to potential transboundary natural disasters, particularly GLOFs. The area's extensive glaciers and abundant snow play a vital role in the water resources of Central Asia's arid zone⁷. The Tianshan Mountains are also the source of numerous rivers, but the vast region shows significant spatial differences.

As depicted in Fig. 1, the Tianshan Mountains can be divided into four distinct mountain districts according to geographical location: Central Tianshan, Western Tianshan, Eastern Tianshan, and Northern Tianshan. The region has an arid and semi-arid climate with high evaporation and low precipitation levels and yearly precipitation of $<300 \text{ mm}$. Despite the aridity of the region, the Randolph Glacier Inventory version (RGI7.0) glacier inventory has identified a significant presence of glaciers, numbering $\sim 26,278$ and covering an area of $14,335.69 \text{ km}^2$. It is worth noting that since 1998, climate change has caused substantial changes across all four Tianshan districts. For instance, the temperature has risen at a rate of $0.36\text{--}0.42 \text{ }^\circ\text{C}/10\text{a}$, which is significantly higher than the global temperature rate or the Northern Hemisphere's rate of temperature change.

Methods

Glacial lake boundary extraction. This paper extracted glacial lake boundaries using the semi-automatic water extraction algorithm of global-local threshold segmentation on the GEE platform^{5,34,35}. The algorithm first binarizes the MNDWI grayscale image based on an initial threshold and then annotates all possible water objects in the study area. Next, it established buffers of the same size for the annotated objects based on the resolution of the remote sensing images. Finally, using the OSTU algorithm, a secondary threshold segmentation was performed on each buffered image to obtain more accurate boundaries of glacial lakes³⁶. Considering the potential impact of the resolution of remote sensing images, we only select lakes with an area $\geq 0.01 \text{ km}^2$.

Considering the impact of terrain shadows and cloud coverage on images extracted images of glacial lakes boundaries, we applied a slope threshold of 20° and a shadow threshold of 0.25 to eliminate pixels before global-threshold segmentation. We selected only those satellite remote sensing images that had $<5\%$ cloud coverage.

In order to obtain the current and past 30 years' evolution trends of glacial lakes in the Tianshan Mountains of Central Asia, we extracted a dataset of glacial lakes with areas $\geq 0.01 \text{ km}^2$ using Landsat series and Sentinel-2A/B remote sensing images. The images spanned from 1990 to 2023, sampled at five-time nodes (1990, 2000, 2010, 2020, and 2023). Collecting

data enabled us to analyze changes in the lakes' characteristics and construct a comprehensive glacial lake database for the region.

Within the framework of the 1990–2023 study period, the algorithm chose satellite remote sensing images from 1990, 2000, 2010, 2020, and 2023 for extracting glacial lake boundaries. This paper used the Landsat 4–5 Thematic Mapper (TM) remote sensing imagery to ascertain the boundaries of glacial lakes for the year 1990. Furthermore, the Landsat 7/8 OLI images with a spatial resolution of 30 m were used to ascertain the boundaries of glacial lakes for the years 2000 and 2010; the boundaries of glacial lakes for the years 2020 and 2023 were extracted using Sentinel-2A/B MSI images with a spatial resolution of 10 m. To minimize the effect of seasonal snow and glaciers on high-altitude glacial lake data mapping, image data from the warmest seasons (June to September) were selected. After the extraction was completed, the auto-generated results were carefully verified and proofread using satellite images, online maps, and other available RGI7.0 glacial lake cataloging datasets. The incorrectly extracted parts were then eliminated and the inaccurate parts were manually corrected. To ensure the accuracy and completeness of the glacial lake data and considering the accuracy of the glacier cataloging data, the data were visually inspected and some of the missing glacial lakes were supplemented. Finally, the glacial lakes were compared on ArcMap and the data interactively inspected.

The process of extracting glacial lake boundaries can be plagued by numerous uncertainties, including the quality of the remote sensing image itself (e.g., spatial resolution, cloud coverage, terrain shadow interference, etc.). Some scholars have already studied the interpretation of remote sensing data and the selection of the minimum lake area threshold^{37,38}. Based on previous Landsat research, they found that the glacial lake boundary can be extracted from 30 m Landsat satellite images, and the resolution can be further improved to 15 m through image fusion. It was observed that the area uncertainty caused by remote sensing itself was ± 0.5 pixels^{37,39}. The present study proposes a method for estimating area uncertainty based on Hanshaw and Bookhagen's approach⁴⁰. The uncertainty in calculating the area of the glacial lake can thus be expressed as:

$$\delta = \frac{P}{G} \times \frac{G^2}{2} \times 0.6872 \quad (1)$$

where P is the perimeter of the glacial lake (m) and G is the spatial resolution of the satellite image used for glacial lake extraction (m).

After calculating the uncertainty area, we determined that the area uncertainty of the extracted remote sensing images was $<3.5\%$.

Glacial lake area and volume. We selected five-time windows (1990 ± 1 , 2000 ± 1 , 2010 ± 1 , 2020 ± 1 , and 2023 ± 1) to reveal the current status of glacial lakes in alpine mountainous and their changes over the past 30 years. The area was calculated using the Transverse Mercator projection coordinate system (UTM). The utilized formula estimates the uncertainty and change rate of the number and area of glacial lakes for different periods. The uncertainty of the glacial lake area change rate and area change can be formulated as follows:

$$R = \frac{A_2 - A_1}{A_1} \times 100\% \quad (2)$$

where R is the relative change rate of the glacial lake area, and A_1 and A_2 are the glacial lake areas at the first and last time points, respectively.

The uncertainty of area change can be formulated as:

$$\delta R = \sqrt{\left(\frac{\delta A}{A_2 - A_1}\right)^2 + \left(\frac{\delta A_1}{A_1}\right)^2} \times R \quad (3)$$

where R is the uncertainty of the glacier-lake change, and A_1 and A_2 are the uncertainties of the glacier-lake area at two time points, respectively: $\delta A = \sqrt{\delta A_1 + \delta A_2}$.

The volume of the glacial lake can be calculated as^{6,41}:

$$V = 0.104 \times A^{1.42} \quad (4)$$

where V is the volume of the glacial lake (km^3), and A is the area of the glacial lake (km^2).

Classification of glacial lake types. Different types of glacial lakes undergo different changes. To distinguish between the various types of glacial lake changes, while also considering the complexity of the terrain and the temporal sequence of the images, we categorized moraine lakes and other dammed glacial lakes according to dam type (Fig. 11). A moraine lake refers to a glacial lake with a moraine as the main dam body of the lake. Depending on the location of the glacial lake, it usually involves terminal moraine lakes and lateral moraine lakes. Other dam types of glacial lakes include glacier erosion lakes, landslide-dammed lakes, and bedrock dam lakes (Table 5).

Glacial lake types can be identified using ArcMap and remote sensing images. For specific identification, the obtained glacial lake vector data first needs to be converted into KML format and then superimposed on Google Earth with a high spatial resolution and online images. Finally, the dam body of each glacial lake needs to be identified through the Google Earth 3D model. To do this, we used ArcMap to assign attribute values to glacial lakes. We identified 2474 moraine lakes with an area of $87.95 \pm 0.1 \text{ km}^2$, mainly distributed in the Central and Western Tianshan. We also identified 2083 non-moraine lakes with an area of 117.79 km^2 . This study mainly conducted risk research on future GLOFs in moraine lakes.

Prediction of future glacial lake dynamic changes. Ice-bed topography (DEM without glacier coverage) was used to model the potential location of glacial lakes. We utilized glacier thickness data²⁸ and a digital elevation model (AW3D30 V) with a spatial resolution of 30 m to detect the depressed areas in the ice bed under different scenarios as the potential location and evolution direction of the future glacial lake. Future glacial lake trends in the Tianshan region in 2050 and 2100 were projected by combining three different CO_2 emission scenarios (RCP2.6, RCP4.5, RCP8.5) and assuming a scenario in which the glacier disappears completely⁴⁰.

Glacial lake risk assessment and verification. To quantitatively assessment the risk of GLOFs, an improved GLOF model was used to evaluate the risk and hazard values of glacial lakes in the Central Asian Tianshan region in 2023. The model was verified based on the GLOF events that have already occurred. Since the 1840s, the main source of GLOFs in the Tianshan region has been moraine-dammed glacial lakes; different types of glacial lakes have caused GLOFs as follows: glacial moraine-dammed lakes have caused 120 instances; ice-dammed lakes have caused 93 instances, with the most of them occur in Merzbacher Glacial Lake; supraglacial lakes have caused 19 instances. Overall, moraine-dammed glacial lakes have dominated the types of glacial lakes that have breached. Although glacial ice-dammed lakes contribute to the majority of the breaching events, this is mainly due to the high recurrence and frequent breaching characteristics of glacial ice-dammed lakes.

Since the model does not apply to glacial lakes covered by moraines or located on the side of glaciers, such glacial lakes were not included in this study. The model includes three indices: the hazard index, which represents the likelihood and potential for glacial lake outburst; the exposure index, which represents the extent to which residents and infrastructure in downstream areas may be affected by flooding; and the risk index, which is a function of both the hazard and exposure indices³⁶.

The hazard index combines the four factors: dam slope, topographic potential, glacial lake volume, and the watershed area of the glacial lake. The exposure index considers the potential impacts of a GLOF disaster on communities located downstream, including populations, livestock, roads, natural landscapes, and historic sites. It is used to characterize the areas that may be affected within the range of potentially threatening GLOF runoff (Table 6).

Table 5 | The classification system II of glacial lakes (ICIMOD, 2011; ICIMOD, 2018)

Number	Name	Definition
1	Bedrock-dammed glacial lake	Lakes formed by water accumulation in depressions created by early glacial erosion processes after the glacier has retreated or melted away
1.1	Cirque lake	Lake formed in cirques
1.2	Other glacially eroded lakes	Lakes formed by water accumulation in depressions created by the glacial erosion process, typically located in valleys with gentle slopes
2	Ice-blocked lake	Lakes formed by glacial blockage, including supraglacial lakes or those blocked by the main or tributary glaciers, as well as lakes located between the edges of glaciers and valleys or at the junction of two glaciers
2.1	Supraglacial lake	Lakes formed by glacial moraine blockage after glacier retreat
2.2	Glacial tributaries blocking the lake	Lakes formed by glacial blockage (without lateral moraines), located on one side of the glacier and blocked by the glacier's edge and the valley
3	Moraine-dammed lake	Lakes formed by glacial moraine blockage after glacier retreat
3.1	End moraine-dammed lake	Lakes formed by the blockage of terminal moraine ridges at the glacier's terminus. They are typically in contact with lateral moraine ridges, and the lake water is usually (but not necessarily) in contact with the glacier or has an ice body at the bottom
3.2	Lateral moraine-dammed lake	Lakes formed by the blockage of lateral glacial till. The lakes are typically blocked by the outer side of the lateral moraine ridges, which means they are situated away from the previous path of the glacier
3.3	Ice-dammed moraine blocks lake	Lakes formed by blockage of other moraines (including pot lakes and hot rock lakes)
4	Other glacial lakes	Lakes formed in glacial valleys that are fed by glacial, snow, and permafrost meltwater, but whose damming materials are not direct products of glacial processes, such as debris flows, alluvial deposits, or landslides

Table 6 | OpenStreetMap features used to characterize exposure levels to potential GLOFs

Features	Description
Airport infrastructure	Primarily related to airports, airfields, and other ground facilities that support the operation of airplanes and helicopters
Convenience facility	They are used for mapping facilities for the use of tourists and residents. For example: toilets, telephones, banks, pharmacies, cafes, parking lots, and schools
Buildings	They were used to identify individual buildings or groups of connected buildings
Geology	They were used to describe the geological composition of an area
Air transportation	Used to mark the transportation of people or goods via overhead electrical wires in various forms. For example, these may include cable cars, chairlifts, and drag lifts
Highways and roads	Used to describe roads and sidewalks
Historical sites	Used to describe various historical sites. For example: archeological sites, shipwrecks, ruins, castles, and ancient buildings
Recreation facilities	Used to mark recreational and sports facilities
Man-made landscapes	Used to identify manufactured (artificial) structures added to the landscape
Offices	Offices are business premises where administrative or professional work is conducted
Power facilities	Used to depict the systems for power generation and distribution
Public transport	Related to public transportation. For example: train stations, bus stations, and services
Railway	Includes all types of railroads, from heavily used mainline railroads to an abandoned rail line
Store	Store labels are used as a place of business with stock items for sale
Residential area	Provides detailed information mainly on settlements
Tourism	These may include places to visit, places to stay, and the things and places that provide support
Sports field	Used to provide information about which sports are housed in a facility, such as a sports field or stadium
Nature	Used to describe the natural and physical characteristics of the land
Water	A collective term for bodies of water such as rivers, lakes, seas, groundwater, glaciers, etc.

After all the above impact factors were calculated, the impact factors of all glacial lakes were normalized to 0–1 using the percentage ranking method. The final hazard value of each glacial lake was calculated, assuming equal weights of 0.25 for these factors as triggers of glacial lake outburst hazards¹⁶.

We then divided the final hazard and risk values of all glacial lakes into the five classes of very low, low, medium, high, and very high using the natural partitioning method. We analyzed these values based on the accumulation of all glacial lake hazard values across different regions. To assess future Glacial Lake GLOF risks and hazards in the Tianshan Mountains, we applied the same methodology and then assessed the reliability of the model by the results of glacial lakes that experienced outburst floods in the past.

Data availability

The Landsat images can be downloaded from the United States Geological Survey (USGS) website (<https://glovis.usgs.gov/>). The Sentinel images can be free available at <https://dataspace.copernicus.eu/>. The Randolph Glacier Inventory 7.0 data can be downloaded at <http://www.glims.org/RGI>. The Advanced Land Observing Satellite (ALOS) Global Digital Surface Model (AW3D30 v2.2) is available for download at <https://www.eorc.jaxa.jp/ALOS/en/aw3d30/index.htm>. The Multi-Error-Removed Improved-Terrain (MERIT) DEM is freely available at http://hydro.iis.u-tokyo.ac.jp/~yamada1/MERIT_DEM. The OpenStreetMap data are freely obtained from <http://www.openstreetmap.org>. The CRU TS dataset is available from

the Centre for National Centre for Atmospheric Science (NCAS) at <https://crudata.uea.ac.uk/cru/data/hrg/>.

Code availability

The mapped glacial lake dataset for the Tianshan region for the years 1990–2023 and a detailed list of GLOF events for the years 1984–2019 is available through Zenodo website at <https://zenodo.org/records/13208655>.

Received: 18 May 2024; Accepted: 23 August 2024;

Published online: 07 September 2024

References

1. Veh, G., Korup, O. & Walz, A. Hazard from Himalayan glacier lake outburst floods. *Proc. Natl. Acad. Sci. USA* **117**, 907–912 (2020).
2. Taylor, C., Robinson, T. R., Dunning, S., Rachel Carr, J. & Westoby, M. Glacial lake outburst floods threaten millions globally. *Nat. Commun.* **14**, 487 (2023).
3. Mir, R. A., Jain, S. K., Lohani, A. K. & Saraf, A. K. Glacier recession and glacial lake outburst flood studies in Zanskar basin, western Himalaya. *J. Hydrol.* **564**, 376–396 (2018).
4. Shrestha, F. et al. A comprehensive and version-controlled database of glacial lake outburst floods in High Mountain Asia. *Earth Syst. Sci. Data* **15**, 3941–3961 (2023).
5. Zhang, G. et al. Automated water classification in the Tibetan Plateau using Chinese GF-1 WFV data. *Photogramm. Eng. Remote Sens.* **83**, 509–519 (2017).
6. Rinzin, S. et al. GLOF hazard, exposure, vulnerability, and risk assessment of potentially dangerous glacial lakes in the Bhutan Himalaya. *J. Hydrol.* **619**, 129311 (2023).
7. Chen, Y., Li, W., Deng, H., Fang, G. & Li, Z. Changes in Central Asia's water tower: past, present and future. *Sci. Rep.* **6**, 35458 (2016).
8. Shugar, D. H. et al. Rapid worldwide growth of glacial lakes since 1990. *Nat. Clim. Change* **10**, 939–945 (2020).
9. Abowarda, A. S. et al. Generating surface soil moisture at 30 m spatial resolution using both data fusion and machine learning toward better water resources management at the field scale. *Remote Sens. Environ.* **255**, 112301 (2021).
10. Barry, R. G. The status of research on glaciers and global glacier recession: a review. *Prog. Phys. Geogr. Earth Environ.* **30**, 285–306 (2006).
11. Bolch, T. et al. Identification of potentially dangerous glacial lakes in the northern Tien Shan. *Nat. Hazards* **59**, 1691–1714 (2011).
12. Kirschbaum, D. et al. The state of remote sensing capabilities of cascading hazards over High Mountain Asia. *Front. Earth Sci.* **7**, 197 (2019).
13. Harrison, S. et al. Climate change and the global pattern of moraine-dammed glacial lake outburst floods. *Cryosphere* **12**, 1195–1209 (2018).
14. Bajracharya, B., Shrestha, A. B. & Rajbhandari, L. Glacial lake outburst floods in the Sagarmatha Region: hazard assessment using GIS and hydrodynamic modeling. *Mt. Res. Dev.* **27**, 336–344 (2007).
15. Zhang, G. et al. Characteristics and changes of glacial lakes and outburst floods. *Nat. Rev. Earth Environ.* **5**, 447–462 (2024).
16. Zheng, G. et al. Increasing risk of glacial lake outburst floods from future Third Pole deglaciation. *Nat. Clim. Change* **11**, 411–417 (2021).
17. Bazai, N. A. et al. Increasing glacial lake outburst flood hazard in response to surge glaciers in the Karakoram. *Earth Sci. Rev.* **212**, 103432 (2021).
18. Carrivick, J. L. & Tweed, F. S. A global assessment of the societal impacts of glacier outburst floods. *Glob. Planet. Change* **144**, 1–16 (2016).
19. Carrivick, J. L. & Tweed, F. S. A review of glacier outburst floods in Iceland and Greenland with a megafloods perspective. *Earth Sci. Rev.* **196**, 102876 (2019).
20. Gu, C., Li, S., Liu, M., Hu, K. & Wang, P. Monitoring glacier lake outburst flood (GLOF) of Lake Merzbacher using dense Chinese high-resolution satellite images. *Remote Sens.* **15**, 1941 (2023).
21. Bolch, T. Climate change and glacier retreat in northern Tien Shan (Kazakhstan/Kyrgyzstan) using remote sensing data. *Glob. Planet. Change* **56**, 1–12 (2007).
22. Zaginaev, V. et al. Reconstruction of glacial lake outburst floods in northern Tien Shan: implications for hazard assessment. *Geomorphology* **269**, 75–84 (2016).
23. Zhang, X. et al. Future changes in extreme precipitation from 1.0 °C more warming in the Tianshan Mountains, Central Asia. *J. Hydrol.* **612**, 128269 (2022).
24. Hsieh, P.-F., Lee, L. C. & Chen, N.-Y. Effect of spatial resolution on classification errors of pure and mixed pixels in remote sensing. In *IEEE Transactions on Geoscience and Remote Sensing* Vol. 39, 2657–2663 (IEEE, 2001).
25. Xie, Z., ShangGuan, D., Zhang, S., Ding, Y. & Liu, S. Index for hazard of Glacier Lake Outburst flood of Lake Merzbacher by satellite-based monitoring of lake area and ice cover. *Glob. Planet. Change* **107**, 229–237 (2013).
26. Lenderink, G., Mok, H. Y., Lee, T. C. & Van Oldenborgh, G. J. Scaling and trends of hourly precipitation extremes in two different climate zones – Hong Kong and the Netherlands. *Hydrol. Earth Syst. Sci.* **15**, 3033–3041 (2011).
27. Lin, L. et al. CAM6 simulation of mean and extreme precipitation over Asia: sensitivity to upgraded physical parameterizations and higher horizontal resolution. *Geosci. Model Dev.* **12**, 3773–3793 (2019).
28. Huss, M. & Hock, R. Global-scale hydrological response to future glacier mass loss. *Nat. Clim. Change* **8**, 135–140 (2018).
29. Liu, M., Chen, N., Zhang, Y. & Deng, M. Glacial lake inventory and lake outburst flood/debris flow hazard assessment after the Gorkha earthquake in the Bhote Koshi Basin. *Water* **12**, 464 (2020).
30. Anacona, P. I., Mackintosh, A. & Norton, K. Reconstruction of a glacial lake outburst flood (GLOF) in the Engaño Valley, Chilean Patagonia: lessons for GLOF risk management. *Sci. Total Environ.* **527–528**, 1–11 (2015).
31. Aggarwal, S., Rai, S. C., Thakur, P. K. & Emmer, A. Inventory and recently increasing GLOF susceptibility of glacial lakes in Sikkim, Eastern Himalaya. *Geomorphology* **295**, 39–54 (2017).
32. Winsemius, H. C. et al. Global drivers of future river flood risk. *Nat. Clim. Change* **6**, 381–385 (2016).
33. Cook, K. L., Andermann, C., Gimbert, F., Adhikari, B. R. & Hovius, N. Glacial lake outburst floods as drivers of fluvial erosion in the Himalaya. *Science* **362**, 53–57 (2018).
34. Li, J. & Sheng, Y. An automated scheme for glacial lake dynamics mapping using Landsat imagery and digital elevation models: a case study in the Himalayas. *Int. J. Remote Sens.* **33**, 5194–5213 (2012).
35. Kaushik, S., Rafiq, M., Joshi, P. K. & Singh, T. Examining the glacial lake dynamics in a warming climate and GLOF modelling in parts of Chandra basin, Himachal Pradesh, India. *Sci. Total Environ.* **714**, 136455 (2020).
36. Allen, S. K. Potentially dangerous glacial lakes across the Tibetan Plateau revealed using a large-scale automated assessment approach. *Sci. Bull.* **64**, 435–445 (2019).
37. Wang, X. et al. Changes of glacial lakes and implications in Tian Shan, central Asia, based on remote sensing data from 1990 to 2010. *Environ. Res. Lett.* **8**, 044052 (2013).
38. Zhang, Q. et al. Controls on Alpine Lake Dynamics, Tien Shan, Central Asia. *Remote Sens.* **14**, 4698 (2022).
39. Zhang, G., Yao, T., Xie, H., Wang, W. & Yang, W. An inventory of glacial lakes in the Third Pole region and their changes in response to global warming. *Glob. Planet. Change* **131**, 148–157 (2015).
40. Hanshaw, M. N. & Bookhagen, B. Glacial areas, lake areas, and snow lines from 1975 to 2012: status of the Cordillera Vilcanota, including the Quelccaya Ice Cap, northern central Andes, Peru. *Cryosphere* **8**, 359–376 (2014).

41. Huggel, C., Kääb, A., Haeberli, W., Teyssiere, P. & Paul, F. Remote sensing based assessment of hazards from glacier lake outbursts: a case study in the Swiss Alps. *Can. Geotech. J.* **39**, 316–330 (2002).

Acknowledgements

The Natural Science Foundation of China (42130512, 42071046) and the Strategic Priority Research Program of the Chinese Academy of Sciences (XDB0720402) support the research.

Author contributions

Man Chen: conceptualization, methodology, visualization, writing—original draft. Yaning Chen: conceptualization, methodology, writing—original draft, supervision, funding acquisition, writing—review & editing. Gonghuan Fang: supervision, funding acquisition, writing—review & editing. Guoxiong Zheng: writing—review & editing. Zhi Li: visualization—review in reworked manuscripts, funding acquisition. Yupeng Li: writing—review & editing. Ziyang Zhu: visualization, writing—review & editing.

Competing interests

The authors declare no competing interests.

Additional information

Correspondence and requests for materials should be addressed to Yaning Chen or Gonghuan Fang.

Reprints and permissions information is available at

<http://www.nature.com/reprints>

Publisher's note Springer Nature remains neutral with regard to jurisdictional claims in published maps and institutional affiliations.

Open Access This article is licensed under a Creative Commons Attribution-NonCommercial-NoDerivatives 4.0 International License, which permits any non-commercial use, sharing, distribution and reproduction in any medium or format, as long as you give appropriate credit to the original author(s) and the source, provide a link to the Creative Commons licence, and indicate if you modified the licensed material. You do not have permission under this licence to share adapted material derived from this article or parts of it. The images or other third party material in this article are included in the article's Creative Commons licence, unless indicated otherwise in a credit line to the material. If material is not included in the article's Creative Commons licence and your intended use is not permitted by statutory regulation or exceeds the permitted use, you will need to obtain permission directly from the copyright holder. To view a copy of this licence, visit <http://creativecommons.org/licenses/by-nc-nd/4.0/>.

© The Author(s) 2024